Obstructive sleep apnea aggravates neuroinflammation and pyroptosis in early brain injury following subarachnoid hemorrhage via ASC/HIF-1α pathway

https://doi.org/10.4103/1673-5374.339000

Date of submission: August 31, 2021

Date of decision: November 24, 2021

Date of acceptance: January 17, 2022

Date of web publication: April 1, 2022

Jun Xu[1, #], Qian Li[1, #], Chen-Yu Xu[1], Shan Mao[1], Jia-Jia Jin[1], Wei Gu[1], Ying Shi[1, *], Chun-Fang Zou[1, 2, *], Liang Ye[1, *]

From the Contents

Graphical Abstract *ASC/HIF-1α-mediated regulation of pyroptosis and neuroinflammation after SAH/OSA*

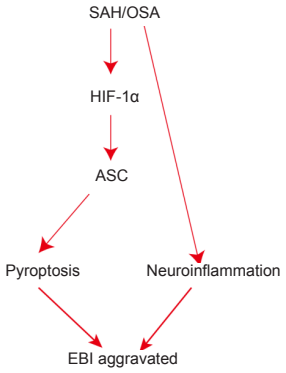

Abstract

Obstructive sleep apnea can worsen the prognosis of subarachnoid hemorrhage. However, the underlying mechanism remains unclear. In this study, we established a mouse model of subarachnoid hemorrhage using the endovascular perforation method and exposed the mice to intermittent hypoxia for 8 hours daily for 2 consecutive days to simulate sleep apnea. We found that sleep apnea aggravated brain edema, increased hippocampal neuron apoptosis, and worsened neurological function in this mouse model of subarachnoid hemorrhage. Then, we established an *in vitro* HT-22 cell model of hemin-induced subarachnoid hemorrhage/intermittent hypoxia and found that the cells died, and lactate dehydrogenase release increased, after 48 hours. We further investigated the underlying mechanism and found that sleep apnea increased the expression of hippocampal neuroinflammatory factors interleukin-1β, interleukin-18, interleukin-6, nuclear factor κB, pyroptosis-related protein caspase-1, pro-caspase-1, and NLRP3, promoted the proliferation of astrocytes, and increased the expression of hypoxia-inducible factor 1α and apoptosis-associated speck-like protein containing a CARD, which are the key proteins in the hypoxia-inducible factor 1α/apoptosis-associated speck-like protein containing a CARD signaling pathway. We also found that knockdown of hypoxia-inducible factor 1α expression *in vitro* greatly reduced the damage to HY22 cells. These findings suggest that sleep apnea aggravates early brain injury after subarachnoid hemorrhage by aggravating neuroinflammation and pyroptosis, at least in part through the hypoxia-inducible factor 1α/apoptosis-associated speck-like protein containing a CARD signaling pathway.

Key Words: apoptosis associated speck like protein containing a CARD; early brain injury; hypoxia-inducible factor 1α; nucleotide-binding domain and leucine-rich repeat protein 3; obstructive sleep apnea; pyroptosis; neuroinflammation; subarachnoid hemorrhage

Introduction

Subarachnoid hemorrhage (SAH) is a very common event that occurs frequently and is associated with high rates of morbidity and mortality, particularly in older patients. The incidence of SAH is 9.1 out of 100,000 persons annually worldwide (95% CI 8.8–9.5), and is higher in Finland, Japan, and China (Ingall et al., 2000; de Rooij et al., 2007; Macdonald and Schweizer, 2017). Previous studies had reported that the short-term mortality rate for SAH ranges between 8.3% and 66.7%, with 8.3% of patients dying before hospital admission, and a survival rate ranging from 36% to 55% (Komotar et al., 2009; Chen et al., 2016b). Most SAH survivors suffer from a long-term emotional impairment, cognitive dysfunction, loss of smell and hearing, and decreased quality of life after surgery (Nieuwkamp et al., 2009). Thus, SAH can impose a substantial burden on the patient's family and on society. Increasing evidence shows that early brain injury (EBI, defined as brain damage occurred within 72 hours after SAH) plays a key role in symptom development following SAH (Chen et al., 2018, 2019). The probable underlying mechanisms for EBI include apoptosis, necroptosis, direct neuronal death, and autophagy (Chen et al., 2016a, 2019; Zhou et al., 2021). Nevertheless, Zille et al. (2017) found that inhibitors of parthanatos, mitophagy, protein or mRNA synthesis, autophagy, or caspase-dependent apoptosis did not affect intracerebral hemorrhage *in vivo* or *in vitro*. Thus, the extent to which various kinds of cell death lead to SAH-induced toxicity remains unclear.

Obstructive sleep apnea (OSA) can induce the formation of intracranial aneurysms, promote aneurysm rupture, aggravate EBI, and worsen the general outcome of patients with vascular aneurysms after SAH (Mason et al., 2011; Chernyshev et al., 2019; Zaremba et al., 2019). In a retrospective analysis, Schuiling et al. (2005) reported that 34% of SAH patients exhibited OSA symptoms, including snoring and more frequent nocturnal awakenings. Bir et al. (2018) also reported that most complications that occur after rupture of an intracranial aneurysm are the consequence of uncontrolled

[1]Department of Respiration, Nanjing First Hospital, Nanjing Medical University, Nanjing, Jiangsu Province, China; [2]Department of Respiration, Nanjing Yuhua Hospital, Yuhua Branch of Nanjing First Hospital, Nanjing, Jiangsu Province, China

*Correspondence to: Ying Shi, PhD, 1339189844@qq.com; Chun-Fang Zou, MD, zouchunfang78@sohu.com; Liang Ye, MD, njyeliang@163.com or yeliang0988@163.com.
https://orcid.org/0000-0002-4648-4448 (Liang Ye)
#Both authors contributed equally to this work.

Funding: *This study was supported by the Natural Science Foundation of Jiangsu Province (Youth Program), No. BK20190129, and National Scientific Program of Jiangsu Colleges and Universities of China, No. 19KJB320012 (both to LY).*

How to cite this article: *Xu J, Li Q, Xu CY, Mao S, Jin JJ, Gu W, Shi Y, Zou CF, Ye L (2022) Obstructive sleep apnea aggravates neuroinflammation and pyroptosis in early brain injury following subarachnoid hemorrhage via ASC/HIF-1α pathway. Neural Regen Res 17(11):2537-2543.*

OSA, and that SAH combined with OSA can aggravate brain injury and lead to a worse outcome. However, the mechanism by which OSA aggravates brain injury remains unclear.

It is unknown whether SAH or OSA leads to hypoxic-ischemic brain injury (Xu et al., 2016; Yu et al., 2019). Xiong et al. (2021) reported that OSA increased oxidative stress and inflammation, then worsened bleomycin-induced pulmonary fibrosis. Hypoxia-inducible factor-1α (HIF-1α) is an important transcription factor whose expression is upregulated in mammals and humans in response to hypoxia or ischemia. Activated HIF-1α enters the nucleus, where it regulates target gene transcription (Xu et al., 2016; Yu et al., 2019). Increasing evidence demonstrates that HIF-1α is significantly upregulated after SAH, and that inhibiting HIF-1α expression can alleviate EBI (Li et al., 2014; Zhaba et al., 2021). In addition, HIF-1α is significantly upregulated in patients with OSA, and hypoxia/ischemia-induced injury is alleviated by HIF-1α inhibition (Yu et al., 2019; Gabryelska et al., 2020). Yu et al. (2019) also reported that hypoxia can induce reactive oxygen species (ROS) overproduction and accumulation, which contribute to cell pyroptosis by activating the HIF-1α and nuclear transcription factor-κB (NF-κB) signaling pathways.

Pyroptosis is a recently recognized mechanism of programmed cell death that has been comprehensively studied which plays a key role in neurological damage (Fricker et al., 2018). Apoptosis-related inhibitors cannot prevent pyroptosis without causing calcium ion overload, which play a vital important role in the EBI after SAH (Chen et al., 2021). In recent years, pyroptosis has been reported to be involved in cerebral hemorrhage, tumors of the central nervous system, and traumatic brain injury (Gao et al., 2020; Lien et al., 2021; Xu et al., 2021b). Yu et al. (2019) demonstrated that pyroptosis is a very important cell death mechanism in hypoxia-induced tissue injury and cell death, particularly in hypoxia-related diseases and OSA. Nonetheless, the exact function of pyroptosis in SAH, and whether it is a viable target for therapy, remains to be verified. Furthermore, a comprehensive investigation of the relationship between OSA on SAH is lacking, and the specific mechanism underlying this relationship is unclear (Mason et al., 2011; Chernyshev et al., 2019; Zaremba et al., 2019). In this study, we explored the function of OSA in EBI following experimentally-induced SAH in mice.

Materials and Methods

Animals

All of the animal experiments carried out as part of this research project adhered to the guidelines stipulated by the National Institutes of Health regarding the care of laboratory animals. Approval for the animal experiments was obtained from the Ethics Committee of the Nanjing Medical University, China on January 15, 2020 (approval No. NYLL-2020-11).

A previous study reported that estrogen levels affect EBI after SAH (Kao et al., 2013). Thus, the animals used for this study were 120 healthy adult male C57BL/6J mice (age 6–8 weeks; weight 22–25 g, Nanjing Medical University, China, license No. SCXK (Su) 2019-00001). The mice were housed in a climate-controlled environment at 25 ± 2°C and 55 ± 5% humidity with 12/12-hour dark/light cycle and unrestricted access to water and food.

Experimental subarachnoid hemorrhage model

The 120 mice were randomly divided into eight groups (15 animals/group): sham, OSA, SAH, SAH + OSA, SAH + si-Con, SAH + si-HIF-1α, SAH + OSA + si-Con, and SAH + OSA + si-HIF-1α. The SAH model was established by the endovascular perforation method, based on a procedure that has been previously described (Chen et al., 2021). To anesthetize the male C57BL6/J mice, pentobarbital sodium (Sigma, St. Louis, MO, USA) was administered via intraperitoneal injection at a dose of 50 mg/kg. The anesthetized animals were placed on a heating pad during the operation to maintain their temperature at 37 ± 0.5°C. A midline incision was made in the neck to expose the left internal and external carotid arteries. The left external carotid artery was then ligated and cut, resulting in a 3-mm stump. A 15-mm-long 4-0 monofilament nylon suture was introduced into the left internal carotid artery via the external carotid artery stump to perforate the cerebral artery at the midpoint and where it bifurcated from the anterior artery. Then, the suture was inserted another 3 mm to induce further perforation at these two sites. The suture was removed after approximately 10 seconds. The sham mice underwent the same surgical procedure without perforation.

Experimental OSA model

After the mice recovered from the SAH surgery, OSA was induced as we described in a previous study (Yu et al., 2019). Briefly, the mice were exposed to 8 hours of intermittent normoxic or hypoxic air conditions each day from the day after the SAH procedure. For the OSA mice, the concentration of oxygen in the mouse compartments was monitored utilizing an O_2 analyzer (Meicheng, Shanghai, China, CY-12C). Manipulation of reoxygenation and hypoxia during the daytime was achieved by varying the concentrations of nitrogen and oxygen. The cycles (30 cycles/hour) of intermittent hypoxia entailed 2 minutes of hypoxia at 7 ± 1% O_2 followed by reoxygenation at 21 ± 0.5% O_2. The control mice were subjected to normoxic air conditions. After 48 hours of atmospheric manipulation, the mice were euthanized.

Assessment of mortality and SAH grade

We evaluated the mortality of the mice 48 hours after SAH/OSA. For the surviving mice, the SAH grade was determined based on a grading system described previously (Sugawara et al., 2008). The scores ranged from 0 to 18, with a higher scores indicating better neurological function. Mice with SAH grading scores below 7 and those with no obvious brain injury were excluded from the following experiments (Sugawara et al., 2008; Chen et al., 2021).

Neurological function assessment

The seriousness of EBI was assessed at 48 hours following SAH utilizing a neurological grading system that we described previously (Chen et al., 2020a). The scoring system comprised six tests and explicit protocols, and is illustrated in **Additional Table 1**. Neurological function scores ranged from 3 to 18. Behavioral assessment was performed for all of the mice in the two cohorts, with higher scores representing better neurological function.

Brain water content measurement

As brain edema is an important factor leading to EBI, brain water content was evaluated utilizing the standard wet-dry technique, as described previously (Chen et al., 2019, 2020a, 2021). The mice were euthanized with 100 mg/kg pentobarbital sodium via intraperitoneal injection 48 hours after SAH/OSA, and whole brains were collected, weighed (to obtain the wet weight) and separated into the brain stem, cerebellum, right cortex, and left cortex. These samples were then dried in an oven (Shanghai Bluepard Instruments Company, Shanghai, China) at 100°C for 24 hours and weighed (to obtain the dry weight). The percentage of brain water content was calculated as follows: (wet weight – dry weight)/wet weight × 100.

TdT-mediated dUTP-biotin nick end labeling assay

A TdT-mediated dUTP-biotin nick end labeling (TUNEL) assay was carried out to evaluate cell death in the brain cortex. The procedure was performed with a TUNEL staining kit according to the manufacturer's instructions (Roche Diagnostics GmbH, Basel, Switzerland; Cat# 1684817). Briefly, 50 μL of TUNEL reaction mixture was added to each slide, which were then incubated in a humidified dark chamber at 37°C for 60 minutes. Next, the slides were incubated with 4′,6-diamidino-2-phenylindole at ambient temperature for 5 minutes in the dark to stain the nuclei. A fluorescence microscope (Carl Zeiss, Jena, Thuringia, Germany) was utilized for imaging. The apoptotic index (%) was calculated as follows: number of TUNEL-positive cells/total number of cells × 100.

Cytokine measurements

48 hours after SAH/OSA, interleukin (IL)-1β (Abcam, Cambridge, MA, USA, Cat# ab197742), IL-18 (Abcam, Cat# ab216165), IL-6 (Abcam, Cat# ab222503), and NF-κB (Abcam, Cat# ab176663) levels in the cerebral cortex were evaluated by enzyme-linked immunosorbent assay according to the manufacturer's instructions.

Mouse treatment and cell transfection with small interfering RNA

Pentobarbital sodium was used to anesthetize the mice, which were then restrained on a stereotaxic apparatus (Narishige, Tokyo, Japan). Subsequently, a burr hole was created in the left hemisphere utilizing the following coordinates: 1 mm lateral, 0.2 mm posterior, and 2.2 mm below the horizontal plane of the bregma. This was followed by the injection of 5 μL of small interfering RNA (siRNA) into the left lateral ventricle at a rate of 0.5 μL per minute. To promote the silencing effect, the siRNA was injected 48 hours before SAH. Cell transfection was performed utilizing Lipofectamine RNAiMax reagent (Thermo Fisher Scientific, Waltham, MA, USA) in Opti-MEM medium according to the manufacturer's instructions. The sequences of the targeted siRNA and control siRNAs, which were manufactured by JiKai (Shanghai, China), were as follows: si-HIF-1α sense, 5′-GCU GUU CAC UAA AGU GGA AUC-3′; negative control siRNA sense, 5′-UUC UCC GAA CGU GUC ACG UTT-3′.

Cultured cell lines

All cell lines were cultured as described previously (Chen et al., 2021). HT-22 cells (RRID:CVCL_0321) were provided by Anhui Medical University (Wuxi, China). HT-22 cells were cultured at 37°C with a CO_2 concentration of 5% in Dulbecco's modified Eagle's medium, 10% fetal bovine serum (Gibco, Thermo Fisher Scientific), and 1% penicillin-streptomycin. These experiments were carried out at a cell density ranging between 60% and 80%. The HT-22 cells were authenticated by sensitivity to hemin-induced damage and visually assessed morphology (Alim et al., 2019). All cell lines used in these experiments had been passaged less than 25 times.

HT-22 SAH model

For the HT-22 SAH experiments, hemin (20 to 140 mM for 48 hours; Cat# H9039, Sigma) was used to induce HT-22 cell death. The hemin was dissolved in 0.1 M NaOH. Cells grown to 60% to 70% confluency were treated with 80 mM hemin (in NaOH, median lethal dose, LD50) dissolved in ddH2O. Dimethyl sulfoxide was added to the hemin solution at a final concentration of 80 mM, and the combined solution was sterilized by passing it through a 0.22-μm filter before applying it to the cells. After 48 hours of treatment, the HT-22 cells were washed with phosphate-buffered saline (PBS) pre-warmed to 37°C and evaluated by 3-(4,5-dimethylthiazol-2-yl)-2,5-diphenyl tetrazolium bromide (MTT) assay and dead/live assay to assess cell viability, according to the assay manufacturers' instructions (Promega, Madison, WI, USA). As reported previously, treating neurons with 80 mM hemin for 48 hours imitates SAH or intracranial hemorrhage conditions (Alim et al., 2019).

MTT assay

Cell viability was assessed by MTT assay. HT-22 cells were seeded into 96-well plates, followed by the addition of 20 μL MTT (Sigma) to each well and incubation at 37°C for 4 hours. Then, the culture supernatant was removed,

and the formazan crystals were lysed with dimethylsulfoxide (Sigma) by agitating the plate gently. Afterward, the absorbance at 490 nm was evaluated using a microplate reader (Bio-Rad Laboratories, Hercules, CA, USA), and the results were normalized to the vehicle group.

Dead/live assay

In the case of the dead/live assay, HT-22 cells were washed twice followed by resuspension in PBS. The cells were then treated with calcein-AM (3 μM) and propidium iodide (PI, 4 μM) for 20 minutes in the dark at ambient temperature. Next, the cells were washed and resuspended in PBS and analyzed using a fluorescence microscope system (DMIL 4000B, Leica, Weitzlar, Hesse, Germany). Each experiment was performed in triplicate.

Real-time polymerase chain reaction

Apoptosis-associated speck-like protein containing a CARD (ASC) is an adapter protein encoded by the PYCARD gene that facilitates the assembly of several inflammasomes; first, it forms a caspase-1-activating scaffold, which is followed by the cleavage of pro-caspase-1 to active caspase-1, which ultimately leads to activation of IL-1β and IL-18 and induction of pyroptosis (de Almeida et al., 2015; Liang et al., 2020). HIF-1α plays an important role in neuroinflammation after OSA and SAH (Ostrowski et al., 2005; Xiong et al., 2021). Real-time PCR was used to detect the expression of HIF-1α and ASC. Total RNA was extracted from the fresh left cortex samples obtained 48 hours after SAH/OSA from the cortex samples or from HT-22 cells, using TRIzol reagent according to the manufacturer's instructions. Quantitative real-time polymerase chain reaction (PCR) was performed using standard procedures, as described previously (Chen et al., 2021). Subsequently, reverse transcription of RNA to complementary DNA was performed using a reverse transcription kit (Takara, Kyoto, Japan). mRNA levels were determined by qPCR utilizing SYBR Green Master Mix (Toyobo Co., Ltd., Osaka, Japan). mRNA levels were normalized to glyceraldehyde-3-phosphate dehydrogenase (GAPDH). All analyses were performed in triplicate. The sequences of the primers used to amplify HIF-1α and ASC were as follows: HIF-1α, forward, 5′-GGA CAA GTC ACC ACA GGA CA-3′ and reverse, 5′-GGG AGA AAA TCA AGT CGT GC-3′; ASC, forward, 5′-GGC ACA GCC AGA ACA GAA CA-3′ and reverse, 5′-GCA CGA ACT GCC TGG TAC TG-3′; GAPDH, forward, 5′-TGA TTC TAC CCA CGG CAA GTT-3′ and reverse, 5′-TGA TGG GTT TCC CAT TGA TGA-3′. The $2^{-\Delta\Delta Ct}$ method was used to assess the RNA expression levels (Livak and Schmittgen, 2001).

Lactate dehydrogenase release

In vitro neurotoxicity was ascertained by evaluating the release of lactate dehydrogenase (LDH) using a kit according to the manufacturer's instructions (Jiancheng bioengineer Institute, Nanjing, China). HT-22 cells were collected immediately after SAH/OSA exposure, followed by incubation with the LDH release reagent (Beyotime, Shanghai, China) for 1 hour. After centrifugation at 1000 × *g*, the cell supernatant was combined with an LDH detection reagent (Beyotime) and incubated at room temperature in the dark for 30 minutes. The LDH concentration was quantified (Multiskan MK3, Thermo Fisher Scientific) by measuring the absorbance at 490 nm according to the manufacturer's instructions (Chen et al., 2020b), and the results were normalized to the control group.

Immunohistochemical analysis of glial fibrillary acidic protein

Paraffin-embedded slices of the cerebral cortex were cut into 5-μm-thick sections. After treatment with blocking serum, the sections were incubated with rabbit polyclonal anti-glial fibrillary acidic protein (GFAP; 1:30, Abcam, Cat# ab7260, RRID: AB_305808) antibody overnight at 4°C. After washing with PBS containing Tween-20 three times, the samples were incubated with the secondary antibody at 37°C for 1 hour. Then, 4′,6-diamidino-2-phenylindole (10 μg/mL) was used to stain the nuclei, and images were obtained using a Zeiss fluorescence imaging microscope (Carl Zeiss, Jena, Thuringia, Germany).

Western blot assay

Western blotting was performed to detect pyroptosis-associated proteins, as described previously (Chen et al., 2016a, 2018, 2019, 2020a). Total protein was extracted from HT-22 cells or fresh left cortex samples. The protein concentrations were evaluated by the BCA method (Invitrogen, Waltham, MA, USA). Subsequently, the proteins (50 μg) were resolved on a sodium dodecyl sulfate-polyacrylamide gel and transferred to polyvinylidene fluoride membranes (Millipore, Billerica, MA, USA), followed by blocking with 5% non-fat milk in TBS-T (Tween 20, 0.1%) at 20°C for 1 hour. The membranes were incubated overnight at 4°C with the primary antibodies: rabbit anti-HIF-1α (1:1000, monoclonal, Abcam, Cat# ab179483, RRID: AB_2732807), rabbit anti-pro-caspase-1 p20 (1:1000, Abcam, Cat# ab238972, RRID: AB_2884954), rabbit anti-β-actin (1:1000, polyclonal, Abcam, Cat# ab8227, RRID: AB_2305186), rabbit anti-nucleotide-binding domain leucine-rich repeat pyrin domain containing 3 (NLRP3; 1:1000, Abcam, Cat# ab263899, RRID: AB_2889890), rabbit anti-caspase-1 (1:1000, Abcam, Cat# ab108362, RRID: AB_10858984), and rabbit anti-ASC (1:1000, Cell Signaling Technology, Cat# 67824, RRID: AB_2799736). The membranes were washed with TBS-T three times, and then incubated with goat anti-mouse IgG secondary antibodies (1:5000, Abcam, Cat# ab97035, RRID: AB_10680176) for 90 minutes at 20°C. Quantitative image analysis was performed using ImageJ version 1.52 (Schneider et al., 2012).

Statistical analysis

No statistical methods were used to predetermine sample sizes; however, our sample sizes are similar to those reported in previous publications (Chen et al., 2019, 2021). The evaluator was blinded to the grouping. Nine mice died after the SAH procedure; the rest of the mice were randomly assigned to the groups at up to 15 mice per group. The data are reported as the mean ± standard error of the mean (SEM). SPSS 14.0 (IBM, Armonk, NY, USA) and GraphPad Prism 6 (GraphPad Software, San Diego, CA, USA, www graphpad. com) were used for the statistical analyses. Differences between multiple groups were analyzed using one-way analysis of variance followed by Tukey's *post hoc* test. For all statistical analyses, differences were considered significant at $P < 0.05$.

Results

Mortality and SAH grade after SAH or OSA

Earlier clinical research had reported that OSA can aggravate EBI, increase mortality, and worsen overall outcome in SAH patients (Mason et al., 2011; Chernyshev et al., 2019; Zaremba et al., 2019). Thus, we used the endovascular perforation technique followed by atmospheric manipulation to induce SAH and OSA in mice (**Figure 1A**). We then assessed the influence of OSA on parameters such as SAH grade and survival. As illustrated in **Figure 1**, survival rates were lower in the SAH + OSA cohort, although there was no significant difference compared with the SAH cohort (OR = 0.5, 95% CI: 0.095–2.628, **Figure 1B**). There was no significant difference in SAH grades between the SAH and SAH + OSA groups ($P > 0.05$; **Figure 1C**). Even though OSA did not increase SAH grade or decrease survival, there was a clear trend toward aggravation of both parameters, suggesting a possible correlation that may not have reached statistical significance because of the small sample size.

OSA aggravates EBI following SAH *in vivo*

To elucidate the effects of OSA after SAH on EBI, we measured brain water content 48 hours after SAH to assess brain damage. Compared with the control group, SAH considerably increased the brain water content, and this effect was aggravated by OSA (**Figure 2A**). The neurological scores were lower in the SAH group compared with the sham group, and the SAH + OSA exhibited significantly worse neurological scores compared with the SAH group ($P < 0.05$; **Figure 2B**). To detect hippocampus damage following SAH and OSA, we used the TUNEL assay to quantify cell death 48 hours after injury. As anticipated, there was more hippocampal cell death in the SAH + OSA group than in the SAH group (**Figure 2C**). Taken together, these data show that OSA aggravates EBI after SAH.

OSA aggravates hemin-induced HT-22 cell damage

Given that OSA aggravates EBI *in vivo*, we next sought to elucidate the neuronal damage caused by OSA *in vitro*. Hemin was used to induce SAH, and a cell OSA technique was used to induce OSA (**Figure 1A**). The MTT assay results showed that the rate of neuronal death increased significantly after treatment with hemin, and that this effect was aggravated by OSA (**Figure 3A**). SAH increased LDH release, and OSA enhanced this effect (**Figure 3B**). Furthermore, the results from the dead/live assay illustrated that OSA aggravated hemin-induced HT-22 cell damage (**Figure 3C**).

OSA aggravates neuroinflammation after SAH *in vivo*

Earlier studies have demonstrated that neuroinflammation is a critical feature of EBI following SAH, and that increased neuroinflammation can aggravate EBI (Wei et al., 2020; Chen et al., 2021). The inflammatory complex can induce the release of pro-inflammatory cytokines and/or the initiation of pyroptosis (Chen et al., 2021). Thus, we assessed the hippocampal levels of IL-1β, IL-18, IL-6, and NF-κB by enzyme-linked immunosorbent assay. The results showed that IL-1β, IL-18, IL-6, and NF-κB levels were increased considerably in the SAH group compared with the sham group, whereas levels of pro-inflammatory cytokines were further increased in the OSA + SAH group compared with those in the SAH group ($P < 0.05$; **Figure 4A–D**). Immunohistochemical analysis also illustrated that GFAP expression in the cerebral cortex and astrocyte proliferation increased after SAH, and that OSA aggravated these effects (**Figure 4E**). This suggests that OSA may be aggravated by the elevated levels of pro-inflammatory cytokines, and, at the same, time, OSA may delay clearance of pro-inflammatory cytokines.

OSA aggravates pyroptosis after SAH *in vivo*

Previous studies have indicated that pyroptosis is an important form of cell death in diseases of the central nervous system, and that it also plays an important role in SAH and OSA (Yu et al., 2019; Chen et al., 2021; Xu et al., 2021a). Thus, we next examined the expression of the pyroptosis-associated proteins caspase-1, pro-caspase-1, and NLRP3 following SAH and OSA in fresh left cortex samples by western blot assay (**Figure 5A**). Compared with the sham and OSA groups, caspase-1, pro-caspase-1, and NLRP3 levels were increased in the SAH group ($P < 0.05$; **Figure 5B–D**) and were even higher in the SAH + OSA group ($P < 0.05$; **Figure 5B–D**).

OSA aggravates pyroptosis following SAH via the HIF-1α/ASC signaling pathway *in vivo*

As HIF-1α is vital to both OSA and SAH (Xu et al., 2016; Yu et al., 2019), we hypothesized that activation of the HIF-1α signaling pathway was the main reason for aggravation of pyroptosis by OSA in mice that have experienced SAH. Wu et al. (2020) reported that ASC can modulate HIF-1α stability, thereby modifying the expression levels of NLRP3 inflammasome components. To clarify the potential mechanism of pyroptosis and the role of the HIF-1α/ASC signaling pathway following SAH/OSA, we detected HIF-1α and ASC gene and

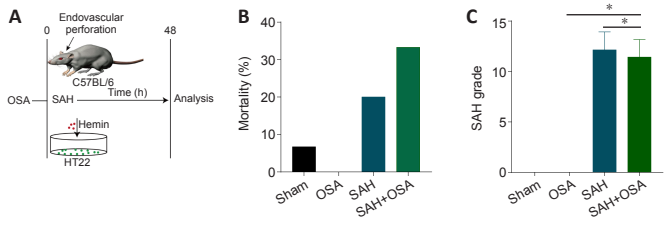

Figure 1 | **Mortality and SAH grade after SAH and OSA.**
(A) Schematic of experimental design for modeling SAH and OSA *in vitro* and *in vivo*. (B) Mortality at 48 hours after surgery. (C) SAH grade at 48 hours after surgery. Higher scores indicate better neurological function. Data are expressed as mean ± SEM (n = 15). *P < 0.05 (one-way analysis of variance followed by Tukey's *post hoc* test). OSA: Obstructive sleep apnea; SAH: subarachnoid hemorrhage.

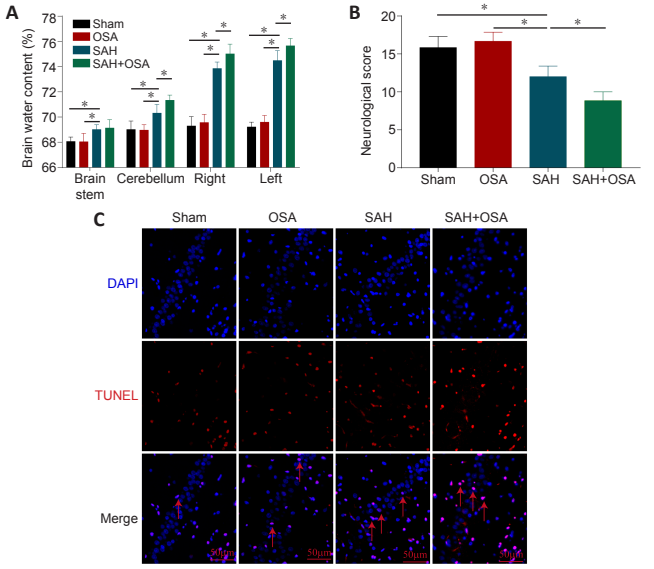

Figure 2 | **OSA aggravates EBI following SAH *in vivo*.**
(A, B) OSA worsens brain edema (A) and neurological behavior scores (B) after SAH. Data are expressed as mean ± SEM (n = 5). *P < 0.05 (one-way analysis of variance followed by Tukey's *post hoc* test). (C) OSA increases hippocampal tissue damage at 48 hours after SAH. Red arrows indicate dead cells. Scale bar: 50 μm. EBI: Early brain injury; OSA: obstructive sleep apnea; SAH: subarachnoid hemorrhage.

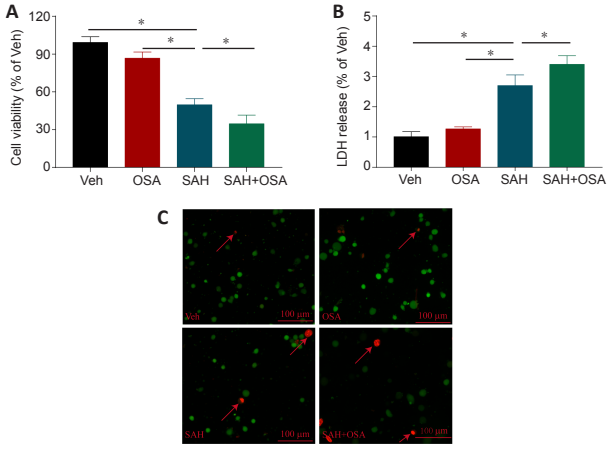

Figure 3 | **OSA increases hemin-induced HT-22 neuronal cell injury *in vitro*.**
(A) MTT assay showing that OSA increases HT-22 neuronal cell death 48 hours following hemin-induced SAH *in vitro*. (B) LDH release assay showing that OSA increases HT-22 neuronal cell death 48 hours following hemin-induced SAH *in vitro*. Data are expressed as mean ± SEM (n = 5). *P < 0.05 (one-way analysis of variance followed by Tukey's *post hoc* test). (C) Live/dead assay showing that OSA aggravates hemin-induced HT-22 neuronal cell death. Red arrows indicate dead cells. Red fluorescence indicates dead cells, and green fluorescence indicates live cells. Scale bars: 100 μm. LDH: Lactate dehydrogenase; MTT: 3-(4,5-dimethylthiazol-2-yl)-2,5-diphenyl tetrazolium bromide; OSA: obstructive sleep apnea; SAH: subarachnoid hemorrhage.

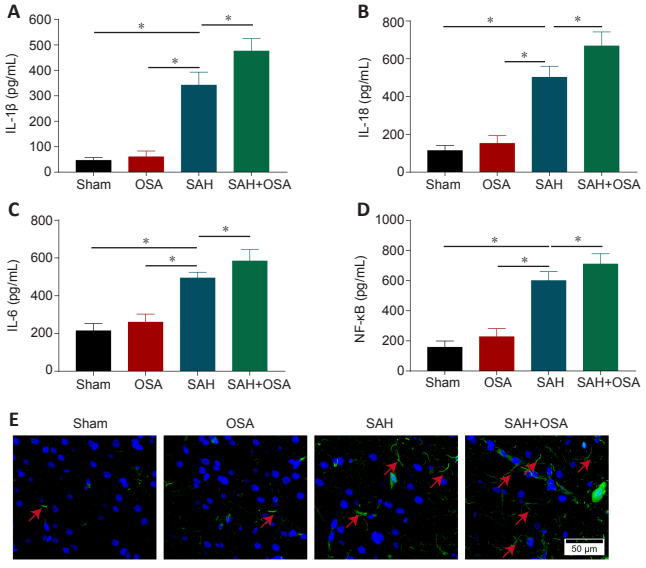

Figure 4 | **OSA aggravates neuroinflammation after SAH *in vivo*.**
(A–D) OSA significantly increases IL-1β (A), IL-18 (B), IL-6 (C), and NF-κB (D) levels in the hippocampus 48 hours following SAH. Data are expressed as mean ± SEM (n = 5). *P < 0.05 (one-way analysis of variance followed by Tukey's *post hoc* test). (E) Immunofluorescence shows that GFAP (green, marked by Alexa Fluor® 488) expression and astrocyte proliferation increased after SAH, and that these effects were aggravated by OSA. Red arrows indicate astrocytes. Scale bar: 50 μm. DAPI: 4′,6-Diamidino-2-phenylindole; GFAP: glial fibrillary acidic protein; IL: interleukin; NF-κB: nuclear transcription factor-κB; OSA: obstructive sleep apnea; SAH: subarachnoid hemorrhage.

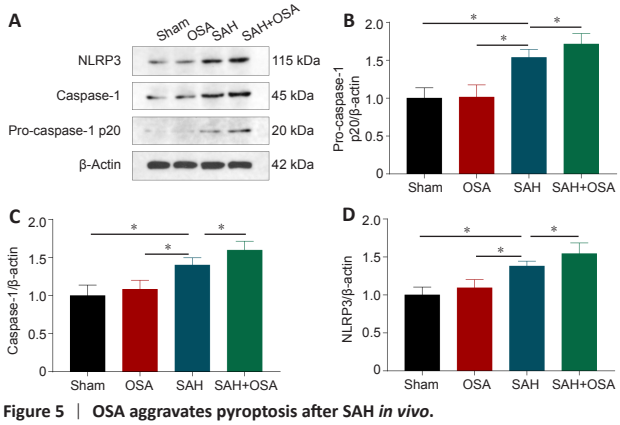

Figure 5 | **OSA aggravates pyroptosis after SAH *in vivo*.**
(A) Detection of NLRP3, pro-caspase-1 p20, and caspase-1 by western blot assay. (B–D) Expression of pro-caspase-1 (B), caspase-1 (C), and NLRP3 (D) (normalized to β-actin) relative to the control. OSA increases pro-caspase-1 p20, caspase-1, and NLRP3 expression following SAH in mice. Data are expressed as mean ± SEM (n = 5). *P < 0.05 (one-way analysis of variance followed by Tukey's *post hoc* test). NLRP3: Nucleotide-binding domain leucine-rich repeat pyrin domain containing 3; OSA: obstructive sleep apnea; SAH: subarachnoid hemorrhage.

protein expression levels in fresh left cortex by real-time PCR and western blot assay, respectively. The results showed that HIF-1α expression was elevated after 48 hours in the SAH group, and was significantly higher in the OSA + SAH group compared with the SAH group (P < 0.05; **Figure 6A** and **B**). ASC and HIF-1α protein expression levels were detected by western blot (**Figure 6C**), which showed that both were increased significantly in the OSA + SAH group compared with the SAH group (P < 0.05; **Figure 6D** and **E**). Hence, OSA promotes EBI after SAH by aggravating pyroptosis, possibly through the HIF-1α/ASC signaling pathway.

Knockdown of HIF-1α alleviates pyroptosis after SAH and OSA *in vitro*
To ascertain the effect of HIF-1α on pyroptosis following SAH/OSA, the expression of pyroptosis-associated proteins was assessed by western blot (**Figure 7A**). Compare with the si-Con group, HIF-1α knockdown considerably reduced the expression of caspase-1, pro-caspase-1, and NLRP3 in the SAH + OSA group (P < 0.05; **Figure 7B–D**). The MTT assay results showed that neuronal death was significantly decreased in the si-HIF-1α group compared with the si-Con group (P < 0.05; **Figure 7E**). Furthermore, LDH release was significantly decreased in the si-HIF-1α group compared with the si-Con group (P < 0.05; **Figure 7F**). The dead/live assay results illustrated that hemin-induced HT-22 cell damage was significantly decreased in the si-HIF-1α group compared with the si-Con group (P < 0.05; **Figure 7G**).

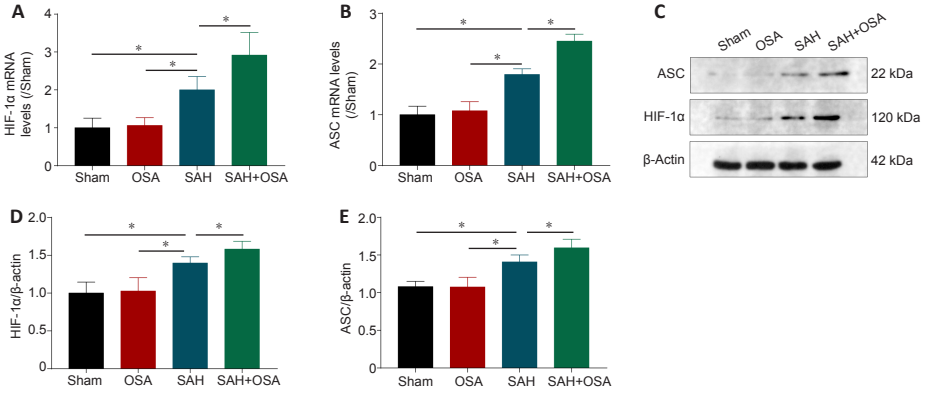

Figure 6 | **OSA aggravates pyroptosis after SAH *in vivo* via the HIF-1α/ASC signaling pathway.**
(A, B) OSA increases HIF-1α (A) and ASC (B) mRNA expression of in the left cortex, as detected by real-time polymerase chain reaction. (C) Detection of HIF-1α and ASC in left cortex samples by western blot. (D, E) HIF-1α (D) and ASC (E) expression (normalized to β-actin) relative to the control. OSA increases HIF-1α expression following SAH in mice. Data are expressed as mean ± SEM (n = 5). *P < 0.05 (one-way analysis of variance followed by Tukey's *post hoc* test). ASC: Apoptosis associated speck like protein containing a CARD; HIF-1α: hypoxia-inducible factor-1α; OSA: obstructive sleep apnea; SAH: subarachnoid hemorrhage.

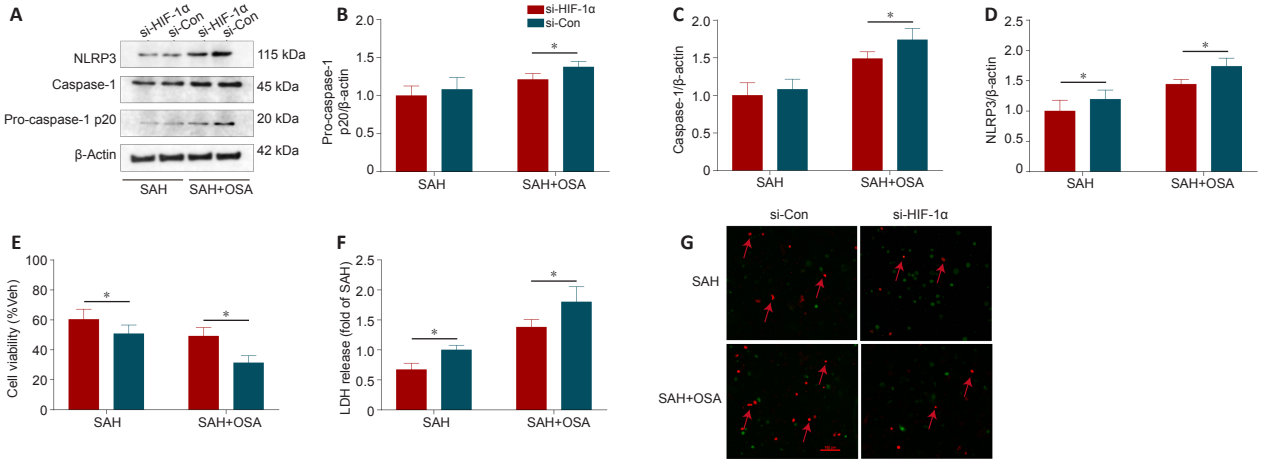

Figure 7 | **HIF-1α knockdown alleviates pyroptosis after SAH/OSA *in vitro*.**
(A) Detection of NLRP3, Pro-caspase-1 p20, and caspase-1 in HT-22 neuronal cells by western blot. (B–D) Pro-caspase-1 (B), caspase-1 (C), and NLRP3 (D) expression (normalized to β-actin) relative to the control. (E) MTT assay showing that HT-22 neuronal cell death decreased significantly after HIF-1α knockdown 48 hours following hemin-induced SAH. (F) LDH release assay showing that HT-22 neuronal cell death decreased significantly after HIF-1α knockdown 48 hours after hemin-induced SAH *in vitro*. Data are expressed as mean ± SEM (n = 5). *P < 0.05 (one-way analysis of variance followed by Tukey's *post hoc* test). (G) Live/dead assay of HT-22 cells exposed to hemin or OSA. HIF-1α knockdown alleviated hemin-induced HT-22 neuronal death. Red arrows indicate dead cells. Scale bar: 100 μm. HIF-1α: Hypoxia-inducible factor-1α; LDH: lactate dehydrogenase; MTT: 3-(4,5-dimethylthiazol-2-yl)-2,5-diphenyl tetrazolium bromide; NLRP3: nucleotide-binding domain leucine-rich repeat pyrin domain containing 3; OSA: obstructive sleep apnea; SAH: subarachnoid hemorrhage.

Knockdown of HIF-1α alleviates EBI after SAH and OSA

To further elucidate the effects of HIF-1α knockdown on EBI in mice that have undergone SAH/OSA, we assessed neurological score, TUNEL assay results, and brain water content at 48 hours following SAH. The results showed that HIF-1α knockdown considerably increased the neurological score compared with that in the si-Con group (P < 0.05; **Figure 8A**). The brain water content was decreased in the HIF-1α knockdown group compared with the si-Con group (P < 0.05; **Figure 8B**). To further assess hippocampal neuron death following HIF-1α knockdown, we performed a TUNEL assay to quantify cell death. As anticipated, less hippocampal tissue damage occurred in the si-HIF-1α group compared with in the si-Con group (**Figure 8C**). These findings suggest that HIF-1α knockdown can alleviate EBI after SAH/OSA *in vivo*.

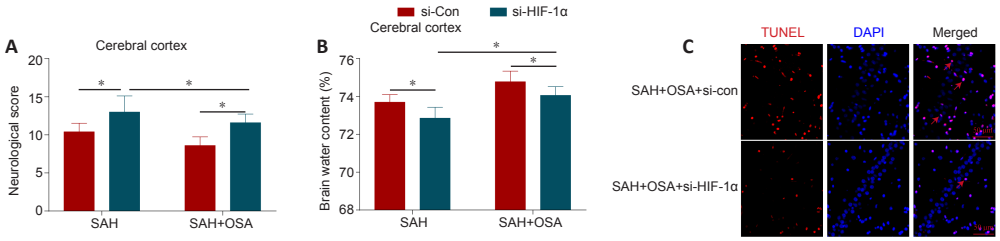

Figure 8 | **HIF-1α knockdown alleviates EBI after SAH and OSA *in vivo*.**
(A) HIF-1α knockdown improved neurological dysfunction after SAH/OSA. (B) HIF-1α knockdown decreased brain edema after SAH/OSA. Data are expressed as mean ± SEM (n = 5)*P < 0.05 (one-way analysis of variance followed by Tukey's *post hoc* test). (C) HIF-1α knockdown decreased hippocampal tissue damage at 48 hours after SAH, as determined by TUNEL staining (red arrows indicate dead cells). Scale bar: 50 μm. DAPI: 4′,6-Diamidino-2-phenylindole, dihydrochloride; EBI: early brain injury; HIF-1α: hypoxia-inducible factor-1α; OSA: obstructive sleep apnea; SAH: subarachnoid hemorrhage; TUNEL: terminal deoxynucleotidyl transferase dUTP nick end labeling.

Discussion

In this study, we found that OSA aggravates EBI in a mouse model of SAH. Specifically: (1) OSA aggravates neurological dysfunction after SAH; (2) OSA enhances brain damage after SAH; (3) OSA promotes neuroinflammation after SAH, thereby increasing inflammatory damage to the brain; (4) OSA can activate pyroptosis after SAH and induce neuronal death; and (5) the mechanism by which OSA aggravates EBI after SAH may be related to the HIF-1α/ASC signaling pathway.

Interruption of breathing by OSA causes intermittent hypoxia, resulting in decreased blood oxygen saturation and impaired sleep quality, and prolonged hypoxia may induce various inflammatory responses that affect the function of the vascular endothelium (Tan et al., 2021). OSA seriously impairs the quality of life of older people and also leads to or aggravates various comorbidities, including hypertension (Prabhakar et al., 2020), coronary heart disease (Strausz et al., 2021), ICH (Orrù et al., 2020), and stroke (Li et al., 2020). The molecular mechanism underlying OSA-induced disease has proven extremely complicated to unravel, and there are several theories that attempt

to explain this process. OSA can induce activation of the inflammatory system, leading to the production of high levels of ROS, and ROS are a probable therapeutic target for alleviating hypoxia-induced tissue injury and cell death (Yu et al., 2019). Furthermore, increasing evidence confirms the relationships between OSA, cognitive impairment, and central nervous system disease (Hung et al., 2008; Pontes-Neto et al., 2010; Mason et al., 2011; Chernyshev et al., 2019; Zaremba et al., 2019; Orrù et al., 2020; Geer et al., 2021).

Chen et al. (2021) reported that inflammasome activation and pyroptosis are largely responsible for the neuronal death and EBI observed in the experimental mouse model of SAH. In *in vivo* and *in vitro* models of SAH, the expression of triggering receptor on myeloid cells can trigger microglial pyroptosis by activating the NLRP3 inflammasome and aggravating neuroinflammation (Xu et al., 2021a). Polarization of microglia is the primary factor that leads to neuroinflammatory damage following stroke. The NLRP1 and NLRP3 inflammasomes, which are members of the NLR inflammasome family, are expressed mainly within the microglia, neurons, and endothelium, and play crucial roles in diseases of the central nervous system (Tan et al., 2014; Lin et al., 2018; Fang et al., 2020). Yuan et al. (2020) also reported that gasdermin D can induce pyroptosis after SAH, that the absent in melanoma 2 (AIM2) inflammasome and AIM2/caspase-1 pathway mediated EBI following SAH, and that the degree of EBI was lessened when AIM2 and caspase-1 were knocked down. In the current study, we found that OSA can activate pyroptosis after SAH and induce neuronal death, and that these effects may be mediated by the HIF-1α/ASC signaling pathway. A previous study also reported that hypoxia or OSA can induce ROS production, which then contributes to pyroptosis via the NF-κB/HIF-1α signaling pathway (Yu et al., 2019).

Similarly, neuroinflammation functions synergistically with pyroptosis in the pathogenesis of OSA/SAH-induced EBI. In a murine model of sleep apnea, the pyroptosis-associated NLRP3 inflammasome was shown to regulate PINK1-Parkin-depended mitophagy, and NLRP3 knockout or inhibition improved neurocognitive function after OSA through alleviating neuroinflammation and enhancing Parkin-mediated mitophagy (Wu et al., 2021). Gong et al. (2020) also reported that OSA causes IH in mice, then leads to neuronal apoptosis and hippocampal neuroinflammation, affecting spatial learning and memory; these effects were, reversed by pinocembrin-mediated inhibition of the NLRP3 inflammasome and promotion of BNIP3 (Bcl-2/adenovirus E1B 19-kDa interacting protein 3)-mediated mitophagy in the hippocampus. Moreover, in an experimental model of diabetes combined with OSA, neuroinflammation and hippocampal neuronal apoptosis were the main reasons for the cognitive deficits that were observed, and these effects were thought to be mediated through the phosphatidylinositol 3-kinase/Akt/glycogen synthase kinase-3β signaling pathway (Shi et al., 2018). Thus, our findings suggest that OSA can aggravate SAH-induced EBI by activating neuroinflammation and pyroptosis.

Although many studies have shown that pyroptosis and neuroinflammation are involved in a variety of diseases of the central nervous system, the mechanisms and molecular networks regulating the interactions between these two processes remained unclear. In this study, we demonstrated that pyroptosis and neuroinflammation lead to neuronal death after SAH/OSA, that neuronal death is aggravated by OSA, and that the mechanism is potentially dependent on the HIF-1α/ASC signaling pathway. Wu et al. (2020) also reported that ASC can modulate HIF-1α stability, causing lymph node metastasis of oral squamous cell carcinoma. A previous study had confirmed that downregulation of the expression of HIF-1α and its target genes can decrease neuronal apoptosis and BBB disruption in an animal model of SAH (Xu et al., 2016). In a mouse model of ischemic stroke, neuron-specific knockout of HIF-1α decreases early acute neurological impairment and neuronal cell death by decreasing apoptosis and increasing angiogenesis (Barteczek et al., 2017). Additionally, multiple previous studies have demonstrated that many neuroprotective drugs can inhibit HIF-1α expression, thereby improving neurological dysfunction, decreasing neuronal death, and reducing blood–brain barrier permeability (Schaible et al., 2014; Trollmann et al., 2014; Min et al., 2015). Hu et al. (2021) reported that a particular synthetic TGR5 agonist, INT-777, can alleviate NLRP3-ASC inflammasome activation and reduce neuroinflammation following SAH. Ystgaard et al. (2019) reported that brain infarction volumes decreased significantly after ASC was knocked out in a neonatal hypoxia-ischemia model. Hence, the HIF-1α/ASC signaling pathway has a crucial function in neuroinflammation and pyroptosis after SAH.

The present study has several limitations. First, we did not determine the precise mechanism of the ASC/HIF-1α axis in regulating pyroptosis. Second, we did not explore the detailed basis of neuroinflammation, such as activation of microglial cells or astrocytes. Finally, it is difficult to accurately evaluate microglial activation using immunofluorescence alone, and additional methods such as flow cytometry may be more suitable and accurate for use in future investigations.

In summary, this study showed that OSA can worsen neurological outcomes, increase brain edema, aggravate neuronal damage, and promote neuronal death in mice that have undergone SAH. These effects are potentially mediated by enhanced neural pyroptosis and neuroinflammation, specifically through the action of ASC and the NLRP3 inflammasome, which is emerging as a crucial cellular regulatory mechanism that contributes to EBI following SAH. This study also showed that OSA aggravates neuroinflammation, pyroptosis, and neuronal death through the HIF-1α/ASC pathway.

Acknowledgments: *We thank Junhui Chen (Anhui Medical University, China) for providing the HT-22 cells.*

Author contributions: *Study design and manuscript revision: LY, JX, CFZ; experiment implementation: LY, JX, CFZ, QL, SM, JJJ, YS, QL, WG; manuscript draft: LY, JX, CFZ; data analysis: LY, JX, QL, SM, YS, QL, WG. All authors read and approved the final manuscript.*

Conflicts of interest: *The authors declare that they have no competing interests.*

Availability of data and materials: *All data generated or analyzed during this study are included in this published article and its supplementary information files.*

Open peer reviewers: *Junfan Chen, The Chinese University of Hong Kong, China; Clarissa Cavarsan, Universidade Federal do Paraná, Brazil.*

Additional files:

Additional Table 1: *Neurological Behavior Scores.*

Additional file 1: *Open peer review reports 1 and 2.*

References

Alim I, Caulfield JT, Chen Y, Swarup V, Geschwind DH, Ivanova E, Seravalli J, Ai Y, Sansing LH, Ste Marie EJ, Hondal RJ, Mukherjee S, Cave JW, Sagdullaev BT, Karuppagounder SS, Ratan RR (2019) Selenium drives a transcriptional adaptive program to block ferroptosis and treat stroke. Cell 177:1262-1279.e25.

Barteczek P, Li L, Ernst AS, Böhler LI, Marti HH, Kunze R (2017) Neuronal HIF-1α and HIF-2α deficiency improves neuronal survival and sensorimotor function in the early acute phase after ischemic stroke. J Cereb Blood Flow Metab 37:291-306.

Bir SC, Nanda A, Cuellar H, Sun H, Guthikonda B, Liendo C, Minagar A, Chernyshev OY (2018) Coexistence of obstructive sleep apnea worsens the overall outcome of intracranial aneurysm: a pioneer study. J Neurosurg 128:735-746.

Chen JH, Yang LK, Chen L, Wang YH, Wu Y, Jiang BJ, Zhu J, Li PP (2016a) Atorvastatin ameliorates early brain injury after subarachnoid hemorrhage via inhibition of AQP4 expression in rabbits. Int J Mol Med 37:1059-1066.

Chen JH, Wu T, Yang LK, Chen L, Zhu J, Li PP, Hu X, Wang YH (2018) Protective effects of atorvastatin on cerebral vessel autoregulation in an experimental rabbit model of subarachnoid hemorrhage. Mol Med Rep 17:1651-1659.

Chen J, Zhu J, He J, Wang Y, Chen L, Zhang C, Zhou J, Yang L (2016b) Ultra-early microsurgical treatment within 24 h of SAH improves prognosis of poor-grade aneurysm combined with intracerebral hematoma. Oncol Lett 11:3173-3178.

Chen J, Zhang C, Yan T, Yang L, Wang Y, Shi Z, Li M, Chen Q (2021) Atorvastatin ameliorates early brain injury after subarachnoid hemorrhage via inhibition of pyroptosis and neuroinflammation. J Cell Physiol 236:6920-6931.

Chen J, Xuan Y, Chen Y, Wu T, Chen L, Guan H, Yang S, He J, Shi D, Wang Y (2019) Netrin-1 alleviates subarachnoid haemorrhage-induced brain injury via the PPARγ/NF-KB signalling pathway. J Cell Mol Med 23:2256-2262.

Chen JH, Wu T, Xia WY, Shi ZH, Zhang CL, Chen L, Chen QX, Wang YH (2020a) An early neuroprotective effect of atorvastatin against subarachnoid hemorrhage. Neural Regen Res 15:1947-1954.

Chen T, Zhu J, Wang YH, Hang CH (2020b) Arc silence aggravates traumatic neuronal injury via mGluR1-mediated ER stress and necroptosis. Cell Death Dis 11:4.

Chernyshev OY, Bir SC, Maiti TK, Patra DP, Sun H, Guthikonda B, Kelley RE, Cuellar H, Minagar A, Nanda A (2019) The relationship between obstructive sleep apnea and ruptured intracranial aneurysms. J Clin Sleep Med 15:1839-1848.

de Almeida L, Khare S, Misharin AV, Patel R, Ratsimandresey RA, Wallin MC, Perlman H, Greaves DR, Hoffman HM, Dorfleutner A, Stehlik C (2015) The PYRIN domain-only protein POP1 inhibits inflammasome assembly and ameliorates inflammatory disease. Immunity 43:264-276.

de Rooij NK, Linn FH, van der Plas JA, Algra A, Rinkel GJ (2007) Incidence of subarachnoid haemorrhage: a systematic review with emphasis on region, age, gender and time trends. J Neurol Neurosurg Psychiatry 78:1365-1372.

Fang Y, Gao S, Wang X, Cao Y, Lu J, Chen S, Lenahan C, Zhang JH, Shao A, Zhang J (2020) Programmed cell deaths and potential crosstalk with blood-brain barrier dysfunction after hemorrhagic stroke. Front Cell Neurosci 14:68.

Fricker M, Tolkovsky AM, Borutaite V, Coleman M, Brown GC (2018) Neuronal cell death. Physiol Rev 98:813-880.

Gabryelska A, Sochal M, Turkiewicz S, Białasiewicz P (2020) Relationship between HIF-1 and circadian clock proteins in obstructive sleep apnea patients-preliminary study. J Clin Med 9:1599.

Gao C, Yan Y, Chen G, Wang T, Luo C, Zhang M, Chen X, Tao L (2020) Autophagy activation represses pyroptosis through the IL-13 and JAK1/STAT1 pathways in a mouse model of moderate traumatic brain injury. ACS Chem Neurosci 11:4231-4239.

Geer JH, Falcone GJ, Vanent KN, Leasure AC, Woo D, Molano JR, Sansing LH, Langefeld CD, Pisani MA, Yaggi HK, Sheth KN (2021) Obstructive sleep apnea as a risk factor for intracerebral hemorrhage. Stroke 52:1835-1838.

Gong LJ, Wang XY, Gu WY, Wu X (2020) Pinocembrin ameliorates intermittent hypoxia-induced neuroinflammation through BNIP3-dependent mitophagy in a murine model of sleep apnea. J Neuroinflammation 17:337.

Hu X, Yan J, Huang L, Araujo C, Peng J, Gao L, Liu S, Tang J, Zuo G, Zhang JH (2021) INT-777 attenuates NLRP3-ASC inflammasome-mediated neuroinflammation via TGR5/cAMP/PKA signaling pathway after subarachnoid hemorrhage in rats. Brain Behav Immun 91:587-600.

Hung MW, Tipoe GL, Poon AM, Reiter RJ, Fung ML (2008) Protective effect of melatonin against hippocampal injury of rats with intermittent hypoxia. J Pineal Res 44:214-221.

Ingall T, Asplund K, Mähönen M, Bonita R (2000) A multinational comparison of subarachnoid hemorrhage epidemiology in the WHO MONICA stroke study. Stroke 31:1054-1061.

Kao CH, Chang CZ, Su YF, Tsai YJ, Chang KP, Lin TK, Hwang SL, Lin CL (2013) 17β-Estradiol attenuates secondary injury through activation of Akt signaling via estrogen receptor alpha in rat brain following subarachnoid hemorrhage. J Surg Res 183:e23-30.

Komotar RJ, Schmidt JM, Starke RM, Claassen J, Wartenberg KE, Lee K, Badjatia N, Connolly ES, Jr., Mayer SA (2009) Resuscitation and critical care of poor-grade subarachnoid hemorrhage. Neurosurgery 64:397-410; discussion 410-411.

Li J, McEvoy RD, Zheng D, Loffler KA, Wang X, Redline S, Woodman RJ, Anderson CS (2020) Self-reported snoring patterns predict stroke events in high-risk patients with OSA: post hoc analyses of the SAVE study. Chest 158:2146-2154.

Li WD, Sun Q, Zhang XS, Wang CX, Li S, Li W, Hang CH (2014) Expression and cell distribution of neuroglobin in the brain tissue after experimental subarachnoid hemorrhage in rats: a pilot study. Cell Mol Neurobiol 34:247-255.

Liang Y, Song P, Chen W, Xie X, Luo R, Su J, Zhu Y, Xu J, Liu R, Zhu P, Zhang Y, Huang M (2020) Inhibition of caspase-1 ameliorates ischemia-associated blood-brain barrier dysfunction and integrity by suppressing pyroptosis activation. Front Cell Neurosci 14:540669.

Lien TS, Sun DS, Wu CY, Chang HH (2021) Exposure to dengue envelope protein domain III induces Nlrp3 inflammasome-dependent endothelial dysfunction and hemorrhage in mice. Front Immunol 12:617251.

Lin X, Ye H, Siaw-Debrah F, Pan S, He Z, Ni H, Xu Z, Jin K, Zhuge Q, Huang L (2018) AC-YVAD-CMK inhibits pyroptosis and improves functional outcome after intracerebral hemorrhage. Biomed Res Int 2018:3706047.

Livak KJ, Schmittgen TD (2001) Analysis of relative gene expression data using real-time quantitative PCR and the 2(-Delta Delta C(T)) Method. Methods 25:402-408.

Macdonald RL, Schweizer TA (2017) Spontaneous subarachnoid haemorrhage. Lancet 389:655-666.

Mason RH, Ruegg G, Perkins J, Hardinge M, Amann-Vesti B, Senn O, Stradling JR, Kohler M (2011) Obstructive sleep apnea in patients with abdominal aortic aneurysms: highly prevalent and associated with aneurysm expansion. Am J Respir Crit Care Med 183:668-674.

Min JW, Hu JJ, He M, Sanchez RM, Huang WX, Liu YQ, Bsoul NB, Han S, Yin J, Liu WH, He XH, Peng BW (2015) Vitexin reduces hypoxia-ischemia neonatal brain injury by the inhibition of HIF-1alpha in a rat pup model. Neuropharmacology 99:38-50.

Nieuwkamp DJ, Setz LE, Algra A, Linn FH, de Rooij NK, Rinkel GJ (2009) Changes in case fatality of aneurysmal subarachnoid haemorrhage over time, according to age, sex, and region: a meta-analysis. Lancet Neurol 8:635-642.

Orrù G, Storari M, Scano A, Piras V, Taibi R, Viscuso D (2020) Obstructive Sleep Apnea, oxidative stress, inflammation and endothelial dysfunction-An overview of predictive laboratory biomarkers. Eur Rev Med Pharmacol Sci 24:6939-6948.

Ostrowski RP, Colohan AR, Zhang JH (2005) Mechanisms of hyperbaric oxygen-induced neuroprotection in a rat model of subarachnoid hemorrhage. J Cereb Blood Flow Metab 25:554-571.

Pontes-Neto OM, Fernandes RM, Sander HH, da Silva LA, Mariano DC, Nobre F, Simão G, de Araujo DB, dos Santos AC, Leite JP (2010) Obstructive sleep apnea is frequent in patients with hypertensive intracerebral hemorrhage and is related to perihematoma edema. Cerebrovasc Dis 29:36-42.

Prabhakar NR, Peng YJ, Nanduri J (2020) Hypoxia-inducible factors and obstructive sleep apnea. J Clin Invest 130:5042-5051.

Schaible EV, Windschügl J, Bobkiewicz W, Kaburov Y, Dangel L, Krämer T, Huang C, Sebastiani A, Luh C, Werner C, Engelhard K, Thal SC, Schäfer MK (2014) 2-Methoxyestradiol confers neuroprotection and inhibits a maladaptive HIF-1α response after traumatic brain injury in mice. J Neurochem 129:940-954.

Schneider CA, Rasband WS, Eliceiri KW (2012) NIH Image to ImageJ: 25 years of image analysis. Nat Methods 9:671-675.

Schuiling WJ, Rinkel GJ, Walchenbach R, de Weerd AW (2005) Disorders of sleep and wake in patients after subarachnoid hemorrhage. Stroke 36:578-582.

Shi Y, Guo X, Zhang J, Zhou H, Sun B, Feng J (2018) DNA binding protein HMGB1 secreted by activated microglia promotes the apoptosis of hippocampal neurons in diabetes complicated with OSA. Brain Behav Immun 73:482-492.

Strausz S, Ruotsalainen S, Ollila HM, Karjalainen J, Kiiskinen T, Reeve M, Kurki M, Mars N, Havulinna AS, Luonsi E, Mansour Aly D, Ahlqvist E, Teder-Laving M, Palta P, Groop L, Mägi R, Mäkitie A, Salomaa V, Bachour A, Tuomi T, et al. (2021) Genetic analysis of obstructive sleep apnoea discovers a strong association with cardiometabolic health. Eur Respir J 57:2003091.

Sugawara T, Ayer R, Jadhav V, Zhang JH (2008) A new grading system evaluating bleeding scale in filament perforation subarachnoid hemorrhage rat model. J Neurosci Methods 167:327-334.

Tan J, Xing H, Sha S, Li J, Miao Y, Zhang Q (2021) Analysis of circulating microvesicles levels and effects of associated factors in elderly patients with obstructive sleep apnea. Front Aging Neurosci 13:609282.

Tan MS, Tan L, Jiang T, Zhu XC, Wang HF, Jia CD, Yu JT (2014) Amyloid-β induces NLRP1-dependent neuronal pyroptosis in models of Alzheimer's disease. Cell Death Dis 5:e1382.

Trollmann R, Richter M, Jung S, Walkinshaw G, Brackmann F (2014) Pharmacologic stabilization of hypoxia-inducible transcription factors protects developing mouse brain from hypoxia-induced apoptotic cell death. Neuroscience 278:327-342.

Wei C, Guo S, Liu W, Jin F, Wei B, Fan H, Su H, Liu J, Zhang N, Fang D, Li G, Shu S, Li X, He X, Zhang X, Duan C (2020) Resolvin D1 ameliorates inflammation-mediated blood-brain barrier disruption after subarachnoid hemorrhage in rats by modulating A20 and NLRP3 inflammasome. Front Pharmacol 11:610734.

Wu CS, Chang IY, Hung JL, Liao WC, Lai YR, Chang KP, Li HP, Chang YS (2020) ASC modulates HIF-1α stability and induces cell mobility in OSCC. Cell Death Dis 11:721.

Wu X, Gong L, Xie L, Gu W, Wang X, Liu Z, Li S (2021) NLRP3 deficiency protects against intermittent hypoxia-induced neuroinflammation and mitochondrial ROS by promoting the PINK1-Parkin pathway of mitophagy in a murine model of sleep apnea. Front Immunol 12:628168.

Xiong M, Zhao Y, Mo H, Yang H, Yue F, Hu K (2021) Intermittent hypoxia increases ROS/HIF-1α 'related oxidative stress and inflammation and worsens bleomycin-induced pulmonary fibrosis in adult male C57BL/6J mice. Int Immunopharmacol 100:108165.

Xu P, Hong Y, Xie Y, Yuan K, Li J, Sun R, Zhang X, Shi X, Li R, Wu J, Liu X, Hu W, Sun W (2021a) TREM-1 exacerbates neuroinflammatory injury via NLRP3 inflammasome-mediated pyroptosis in experimental subarachnoid hemorrhage. Transl Stroke Res 12:643-659.

Xu W, Xu R, Li X, Zhang H, Wang X, Zhu J (2016) Downregulating hypoxia-inducible factor-1α expression with perfluorooctyl-bromide nanoparticles reduces early brain injury following experimental subarachnoid hemorrhage in rats. Am J Transl Res 8:2114-2126.

Xu W, Song C, Wang X, Li Y, Bai X, Liang X, Wu J, Liu J (2021b) Downregulation of miR-155-5p enhances the anti-tumor effect of cetuximab on triple-negative breast cancer cells via inducing cell apoptosis and pyroptosis. Aging (Albany NY) 13:228-240.

Ystgaard MB, Scheffler K, Suganthan R, Bjørås M, Ranheim T, Sagen EL, Halvorsen B, Saugstad OD, Yndestad A (2019) Neuromodulatory effect of NLRP3 and ASC in neonatal hypoxic ischemic encephalopathy. Neonatology 115:355-362.

Yu LM, Zhang WH, Han XX, Li YY, Lu Y, Pan J, Mao JQ, Zhu LY, Deng JJ, Huang W, Liu YH (2019) Hypoxia-induced ROS contribute to myoblast pyroptosis during obstructive sleep apnea via the NF-κB/HIF-1α signaling pathway. Oxid Med Cell Longev 2019:4596368.

Yuan B, Zhou XM, You ZQ, Xu WD, Fan JM, Chen SJ, Han YL, Wu Q, Zhang X (2020) Inhibition of AIM2 inflammasome activation alleviates GSDMD-induced pyroptosis in early brain injury after subarachnoid haemorrhage. Cell Death Dis 11:76.

Zaremba S, Albus L, Schuss P, Vatter H, Klockgether T, Güresir E (2019) Increased risk for subarachnoid hemorrhage in patients with sleep apnea. J Neurol 266:1351-1357.

Zhaba WD, Deji QZ, Deng HJ, Han YL, Gao SQ, Liu XL, Zhou ML (2021) Retinal hypoxia after experimental subarachnoid hemorrhage. Neurosci Lett 742:135554.

Zhou Y, Tao T, Liu G, Gao X, Gao Y, Zhuang Z, Lu Y, Wang H, Li W, Wu L, Zhang D, Hang C (2021) TRAF3 mediates neuronal apoptosis in early brain injury following subarachnoid hemorrhage via targeting TAK1-dependent MAPKs and NF-κB pathways. Cell Death Dis 12:10.

Zille M, Karuppagounder SS, Chen Y, Gough PJ, Bertin J, Finger J, Milner TA, Jonas EA, Ratan RR (2017) Neuronal death after hemorrhagic stroke in vitro and in vivo shares features of ferroptosis and necroptosis. Stroke 48:1033-1043.

P-Reviewers: Chen J, Cavarsan C; C-Editor: Zhao M; S-Editors: Yu J, Li CH; L-Editors: Crow E, Yu J, Song LP; T-Editor: Jia Y

Additional Table 1 Neurological Behavior Scores

Category	Behavior	Score
Spontaneous activity	• Moved around, explored the environment, and approached at least three walls of the cage.	3
	• Slightly affected moved, did not approach all sides, move hesitating, moved to least one upper rim of the cage.	2
	• Severely affected moved,did not rise up at all and barely moved in the cage.	1
	• Did not move at all.	0
Symmetry in the movement of four limbs	• All four limbs extended symmetrically.	3
	• Limbs on left side extended less or more slowly than those on the right.	2
	• Limbs on left side showed minimal movement.	1
	• Forelimb on left side did not move at all.	0
Forepaw outstretching	• Both forelimbs were outstretched, forepaws walked symmetrically.	3
	• Left side outstretched less than the right, and forepaw walking was impaired.	2
	• Left forelimb moved minimally.	1
	• Left forelimb did not move.	0
Climbing	• Climbed easily and gripped tightly to the wire.	3
	• Left side impaired while climbing or did not grip as hard as the right side.	2
	• Failed to climb or tended to circle instead of climbing.	1
Body proprioception	• Reacted by turning head and was equally startled by the	3
	• stimulus on both sides.	2
	• Reacted slowly to stimulus on left side.	1
	• Did not respond to the stimulus placed on the left side.	
Response to vibrissae touch	• Reacted by turning head or was equally startled by the stimulus on both sides.	3
	• Reacted slowly to stimulus on left side.	2
	• Did not respond to stimulus on the left side.	1